METAL FORMING ANALYSIS VIA EULERIAN-LAGRANGIAN FEM WITH ADAPTIVE MESH

M. HOGGE, J.-Ph. PONTHOT

L.T.A.S. - Thermomécanique, Institut de Mécanique
Université de Liège, 21 rue E. Solvay, B-4000 Liège, Belgium

1. Introduction

Metal forming finite element (FE) simulations have always exhibited difficulties while using classical formulations. As a matter of fact, in the Lagrangian formulation (where the FEs are embedded with the material), one has to cope with changing boundary conditions and mesh distorsions which often lead to a complex and expensive remeshing technique. On the contrary, the Eulerian formulation (where the elements are fixed in space) can afford very large material distorsions but the treatment of moving (unknown) boundaries is always critical.

2. The Eulerian-Lagrangian (EL) formulation

In order to overcome problems met by using the preceding formulations, some authors [1-6] have developped a combined Eulerian-Lagrangian formulation. In this new method, elements have nodal point displacements ($\vec{dv}$) that are uncoupled from material displacements ($\vec{du}$) (see fig. 1), so that matter can flow through the elements (as in an Eulerian formulation) whereas their shape can be controlled to prevent unbounded distorsions. This provides much freedom in formulating the mathematical model. It is possible to fix the mesh in space ($\vec{dv}=0$), which leads to an Eulerian formulation, or to attach it to the body ($\vec{dv}=\vec{du}$), thus resulting in a Lagrangian formulation. It is also possible to allow the mesh to move independently from the material (fig. 2). In the latter case, the tangent stiffness matrix resulting from the linearization of the equilibrium equations is, in general, non-symmetric and rectangular, owing to the fact that, for a 3D problem, a reference location exhibits six degrees of freedom (three Lagrangian ones and three Eulerian ones) while only three equations of equilibrium are provided by the Weighted Residual Principle.

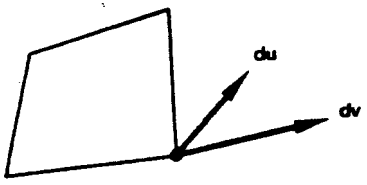

Fig. 1 $\vec{du}$ = material DOF
$\vec{dv}$ = mesh DOF

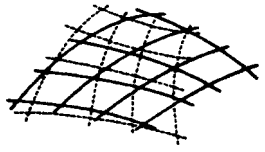

Fig. 2 Dotted line: material
Solid line: mesh

A solvable set of equations can be obtained by generating on the geometry of the deformed body a new mesh (with identical topology and external boundary) as follows :

-first (before deformation), we impose a hierarchical partitioning (fig. 3) of the domain into regions of rather simple geometry: the "MacroRegions" (MR). Each of these MR's is defined, in 2D, by its four (three) sides which are called "Master Lines" (ML). Moreover, each ML is given a physical attribute according to the type of boundary or interMR condition expressed on it. This one can be Eulerian, Lagrangian or Eulerian-Lagrangian. The resulting attribute for a given MR in thus Lagrangian if all ML's are Lagrangian, Eulerian if all ML's are Eulerian and Eulerian-Lagrangian in all other cases.

-second, at each time step, the computation is performed as with an Updated Lagrangian formulation until a new equilibrium position is reached. Then a new mesh is generated by setting :

$\vec{dv} = 0$ for an Eulerian MR
$\vec{dv} = \vec{du}$ for a Lagrangian MR

and using the Transfinite Mapping Method (TMM) [4,5,7] for an EL MR. This technique generates very easily a mesh in an arbitrary 2D domain once a new discretization of the four boundaries has been established (see next paragraph) : internal mesh nodal positions are simply evaluated through a bilinear projector which maps a unit square with uniform mesh onto the true quadrilateral (see fig. 4). We are thus able to generate a mesh in a 2D region with given discretized ML's ; the remaining problem is to adapt the mesh in a 1D manner over each ML so that, for each macroregion, the 2D adaptive problem be replaced by four 1D adaptive problems.

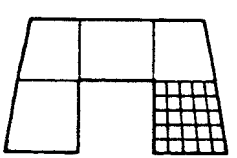

Fig. 3 Hierarchical partitioning

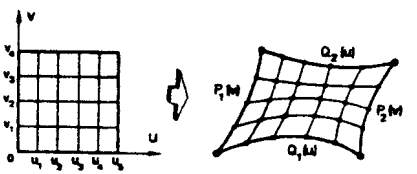

Fig. 4 TMM transformation
(a) reduced domain
(b) physical domain

3. Masterlines 1D nodal relocation

A number of studies on numerical solutions for boundary-value problems in ordinary differential equations [8,9] have shown that the error can be reduced by placing the grid points so that some estimator function be equally distributed over the elements.

Consider the estimator function E(x) and its increment over the grid interval $\Delta x_i = x_{i+1} - x_i$:

$$E(x) = \int_0^x w(u)\, du \qquad (1)$$

$$\Delta E_i^{i+1} = E(x_{i+1}) - E(x_i) = \int_{x_i}^{x_{i+1}} w(u)\, du = \bar{w}_i^{i+1} \cdot \Delta x_i \qquad (2)$$

where w(x) is some positive weight function (WF) and $\bar{w}$ its mean value. The equi-distribution statement requires thus along the ML that :

$$\Delta E_i^{i+1} = \bar{w}_i^{i+1} \cdot \Delta x_i = \text{constant} \qquad (3)$$

With this condition, the grid interval will of course be small where WF is large and vice versa. Thus if WF is some estimation of the error, or of the solution variation, the grid points will be closely spaced in regions of large error, or solution variation, and more widely spaced elsewhere.

Condition (3) over a curve of length L with M points ($x_1 = 0, \ldots, x_M = L$) is met by assuming a new grid position x_i^* such that (see fig. 5) :

$$E(x_i^*) = \frac{i-1}{M-1} E(x_M) \quad (i = 2, \ldots, M-1), \qquad x_1^* = 0 , \qquad x_M^* = L \qquad (4)$$

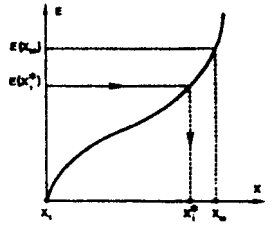

Fig. 5. New grid point position x_i^* insuring equidistributed estimator $E(x_i^*)$.

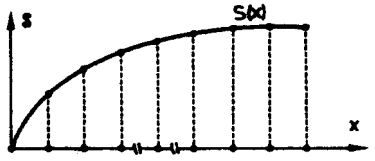

Fig. 6. Equal spacing of grid points.

The selection of an appropriate WF is not obvious. The simplest possible choice is the unit constant w(x) = 1, which leads to equal spacing of all grid points whatever be the solution (see fig. 6), and can give very good results, much better than the Updated Lagrangian formulation, as illustrated in [4, 5, 6].

Clearly more sophisticated WF are needed : the solution gradient, or the gradient of a quantity S related to the solution :

$$w(x) = |S_{,x}| \qquad (5)$$

where the comma denotes a spatial derivative, is a good candidate. With this WF, the nodal point distribution varies so that each grid interval captures the same variation of the solution (see fig. 7),resulting in fine meshing for steep-gradient regions ; on the contrary, if this gradient vanishes, the spacing becomes infinitely large. As a consequence, the regions near extrema, i.e. where $S_{,x} = 0$ locally, need special treatement

(see fig. 8). This can be achieved by incorporating some influence of the second derivative $|S,_{xx}|$ into the WF.

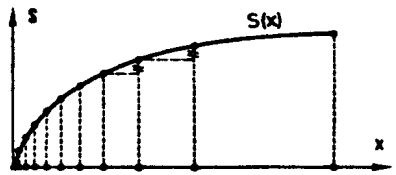

Fig. 7. Equal solution increments.

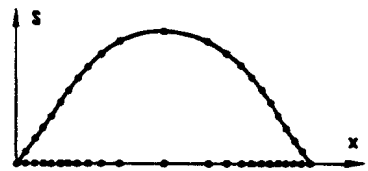

Fig. 8. Large spacing in the region of small solution gradient.

Another interesting quantity in large deformation analysis is an image, no longer of the solution curvature $|S,_{xx}|$, but of the geometrical curvature of the ML arc itself : θ.

A linear combination of the WFs presented above with appropriate norm provides the desired criterion towards concentration in regions of steep gradient/large curvature, near extrema while retaining equal spacing where the solution is constant :

$$w(x) = \frac{1}{L} + \alpha \frac{|S,_x|}{\int_0^L |S,_x| dx} + \beta \frac{|S,_{xx}|}{\int_0^L |S,_{xx}| dx} + \tau \frac{|\theta|}{\int_0^L |\theta| dx} \qquad (6)$$

The non-negative parameters α, β and τ are to be prescribed. Clearly, concentration near steep gradients is emphasized by large values of α, near extrema by large values of β, near high-geometrical curvature by τ while $\alpha = \beta = \tau = 0$ will produce equal point spacing all along the arc.

4. Numerical implementation

In a FEM context with bilinear isoparametric elements, a ML is defined in its discrete form by a set of nodal coordinates linked by straight lines that we shall call "sides". Evaluation of (6) requires the knowledge of the geometrical curvature θ on each side as well as nodal values of S and $S,_x$ (thus resulting on a constant $S,_{xx}$ on each side). We use here $S = \bar{\varepsilon}^p$, the equivalent plastic strain and none of the above required quantity is directly available on the ML's in a kinematically admissible FE model.

The geometrical curvature is evaluated as follows : for each of the (M-1) sides of the ML ($M \geq 3$), consider nodes (i-1) and i bounding the ith side. Consider also a third node, either (i-2) or (i+1), closest to the middle of side i. Then compute the radius R_i of the circle supported by these three nodes. The local curvature is then defined by $\theta_i = 1/R_i$.

As $\bar{\varepsilon}^p$ is a discrete function only known at the FE Gauss points, a continuous

evaluation of $\bar{\varepsilon}^p$ and $\bar{\varepsilon}^p_{,x}$ is more tedious.

First we shall compute a C^0 estimator for $\bar{\varepsilon}^p$ over the domain by assuming for a given element :

$$\bar{\varepsilon}^p(\xi,\eta) = \phi_j(\xi,\eta)\ \bar{\varepsilon}^p_{Nj} \tag{7}$$

where $\phi_j = \frac{1}{4}(1 \pm \xi\,\xi_j)(1 \pm \eta\,\eta_j)$, $(\xi,\eta) \in [-1, 1] \times [-1, 1]$, $(j = 1 \text{ to } 4)$

are the classical shape functions of an isoparametric bilinear element, expressed in natural coordinates and $\bar{\varepsilon}^p_{Nj}$ the (unknown) nodal value of node j with $\xi_j = \mp 1$, $\eta_j = \mp 1$.

If equation (7) is sampled at the four Gauss point (where we precisely know a value of $\bar{\varepsilon}^p$), we get a 4x4 algebraic system with the 4 nodal values of $\bar{\varepsilon}^p$ as unknown quantities :

$$\vec{\varepsilon}_{GP} = \psi \cdot \vec{\varepsilon}_N \tag{8}$$

where

$$\psi_{kj} = \phi_j(\xi_k, \eta_k),\ \vec{\varepsilon}^T_{GP} = \left[\bar{\varepsilon}^p_{GP1}\ \bar{\varepsilon}^p_{GP2}\ \bar{\varepsilon}^p_{GP3}\ \bar{\varepsilon}^p_{GP4}\right],\ \vec{\varepsilon}^T_N = \left[\bar{\varepsilon}^p_{N1}\ \bar{\varepsilon}^p_{N2}\ \bar{\varepsilon}^p_{N3}\ \bar{\varepsilon}^p_{N4}\right] \tag{9}$$

and (ξ_k, η_k) is the location of Gauss Point k, $\xi_k = \mp \frac{1}{\sqrt{3}}$, $\eta_k = \mp \frac{1}{\sqrt{3}}$

Inverting (8) leads to

$$\vec{\varepsilon}_N = \psi^{-1} \cdot \vec{\varepsilon}_{GP} \tag{10}$$

with

$$\psi^{-1} = \begin{bmatrix} \lambda & \mu & \delta & \mu \\ & \lambda & \mu & \delta \\ s & & \lambda & \mu \\ & r & & \lambda \end{bmatrix} \qquad \begin{aligned} \lambda &= 1 + \frac{\sqrt{3}}{2} \\ \mu &= -\frac{1}{2} \\ \delta &= 1 - \frac{\sqrt{3}}{2} \end{aligned} \tag{11}$$

which is identical to the local least square smoothing matrix obtained by Hinton & Campbell [10]. Nodal values for the whole structure are then obtained by a summation of element nodal values of type (10) weighted by the inverse of the number of connecting elements at the given node.

Given this C^0 field of $\bar{\varepsilon}^p$, we can derive a C^{-1} estimator of $\bar{\varepsilon}^p_{,x}$ (piecewise constant on each side) but no one for $\bar{\varepsilon}^p_{,xx}$. Again local or global least square methods [10] could be used in that sake but proved to be unsatisfactory in the present case, leading to strong underestimation of $\bar{\varepsilon}^p_{,x}$ for the limit nodes of the ML (i = 1 & M).

We have thus implemented instead a weighted mean values method [11] yielding a C^0 estimator for $\bar{\varepsilon}^p_{,x}$ from its C^{-1} piecewise variation on each side.

Suppose any scalar quantity σ (i.e. $\bar{\varepsilon}^p_{,x}$ here) exhibits piecewise constant C^{-1} side values $\bar{\sigma}_i$ (i = 1, .., M-1), then the associate C^0 internal nodal values σ^n_i are taken as

$$\sigma^n_i = \omega\, \bar{\sigma}_{i-1} + (1 - \omega)\, \bar{\sigma}_i \qquad (i = 2, \ldots, M-1) \qquad (12)$$

where $$\omega = \Delta x_i / (\Delta x_i + \Delta x_{i-1}) \qquad (13)$$

and the limiting nodal values are extrapoled as (see fig. 9) :

$$\sigma^n_1 = 2\, \bar{\sigma}_1 - \sigma^n_2 \qquad (14)$$

$$\sigma^n_M = 2\, \bar{\sigma}_{M-1} - \sigma^n_{M-1} \qquad (15)$$

Once this C^0 estimator for $\bar{\varepsilon}^p_{,x}$ has been built, the weighting function (6) is available and new grid point positions are determined according to (4) with a piecewise linear estimator function E(x).

A final nodal slide is however often required to insure smooth variation of side lengths along a given ML ; this is done by setting in reverse order

$$x^{n*}_i = (x^n_{i-1} + x^n_{i+1})/2 \qquad (i = M-1, \ldots, 2) \qquad (16)$$

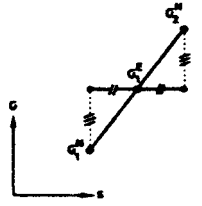

Fig. 9. Extrapolation to obtain a limiting nodal value

5. Numerical example

The EL formulation has already been applied successfully to the simulation of the coining process [1,4], with obvious benefits over standard UL models. However it was never applied before, to our knowledge, in conjunction with an adaptive remeshing technique. The physical situation is displayed on fig. 10 : a 4 mm-wide die, assumed to be rigid, is moving downwards with a prescribed displacement. The body to be formed is a 3 m x 10 mm rectangle with an initial mesh of 24 plus 48 quadrilateral elements. Due to symmetry only a quarter of the specimen is actually modelled. The hierarchical partition consists of 2 MR's : the dark one, always containing the material domain instantaneously located under the punch, and the white one, containing the remaining piece of matter. On the upper moving boundary of this

second MR, the mesh is automatically adapted on the ML with adaptive parameters given by $\alpha = 2$, $\beta = 1$, $\tau = 5$. The lower boundary is a mirror ML of the upper one, while the vertical ML's are EL with equal point spacings (with respect to their relative lengths). The material is J2 elasto-plastic with linear isotropic hardening ($E = 2.1\ 10^5$ N/mm^2 ; $\nu = 0.3$, $\sigma_0 = 250$ N/mm^2; $h = 10^4$ N/mm^2) and all contact areas are assumed to be frictionless.

Adaptive mesh deformation and effective plastic strain patterns are displayed on fig. 11 for 30 % and 60 % height reduction. The latter required 56 computational steps and 4 min 56 sec on a 3 Mips computer, and exhibits adequate capturing of the strain gradient via, the adaptive mesh strategy.

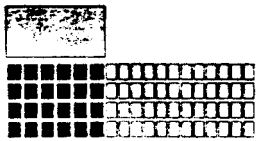

Fig. 10. Initial geometry and Hierarchical Partioning.

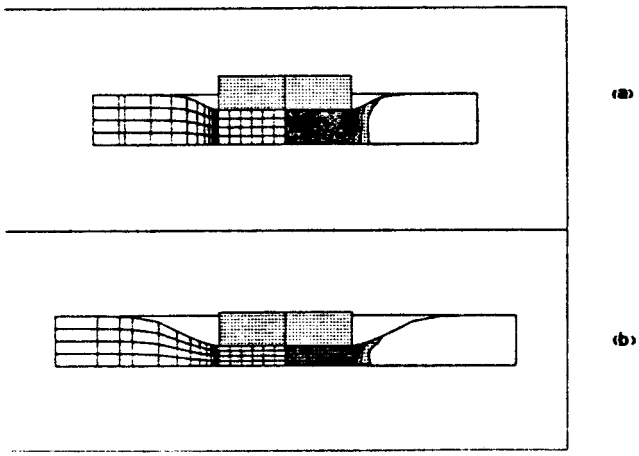

Fig. 11. Mesh and effective plastic strain after 30 % (a) & 60 % (b) height reduction.

6. References

1. Schreurs P., Veldpaus F. & Brekelmans W."Simulation of Forming Processes using the Arbitrary Eulerian-Lagrangian Formulation", Comp. Meth. in App. Mech. and Eng., 58 (1986), 19-36.

2. Huetink J. "Analysis of Metal Forming Processes based on a combined Eulerian-Lagrangian FE Formulation" in "Numerical Methods in Industrial Forming Processes", Swansea, UK, 1982 , pp. 501-509.

3. Cescutti J.P. and Chenot J.L. "A Geometrical Continuous Remeshing Procedure for Application to FE Calculation of Non-steady State Forming Processes" in Proc. of NUMETA'87, SWANSEA, UK, S17.

4. Ponthot J.P. "A Method to Reduce Cost of Mesh Deformation in Eulerian-Lagrangian Form." Proc. of EUROMECH 233, Sophia-Antipolis, France, August 1988, pp. 65-74.

5. Ponthot J.P. "Efficient Mesh Management in Eulerian-Lagrangian Method for Large Deformations Analysis" Proc. of NUMIFORM'89, June 1989, Colorado State Univ., Fort Collins, USA, pp 203-210.

6. Ponthot J.P. "Metal Forming Simulation via Eulerian-Lagrangian FEM with Contact Problems". Proc. of NUMETA'90, Swansea UK, 329-338.

7. Haber, R.; Shepard, M.S.; Abel, J.F.; Gallagher, R.H. and Greenberg, D.P.. "A general two-dimensional, graphical finite element prer-processor utilizing discrete transfinite mappings". Int. J. for Num. Methods in Engineering, Vol. 17, pp. 1015-1044 (1981).

8. Thompson, J.F.; Warsi, Z.V.A. & Mastin, C.W. "Numerical Grid Generation Foundations and Applications". North-Holland (1985).

9. Gerrekens, P. (1988 & 1989). Private communications.

10. Hinton, E.; Campbell L. "Local and Global smoothing of discontinuous finite element functions using a least square method". Int. J. Num. Meth. in E., Vol. 8, pp. 461-480 (1974).

11. Zhong, H.G. & Beckers, P. "Solution Approximation error estimator for the FE solution". 2° Colloque National Belge de Mécanique Théorique et Appliquée, Bruxelles 17-18 mai (1990). Internal Report SA-140, LTAS, University of Liège.